

# PyGLImER: A New Modular Software Suite to Image Crustal and Upper-Mantle Discontinuities Using a Global Database of Ps and Sp Receiver Functions

Peter Makus<sup>1</sup>, Stéphane Rondenay<sup>2</sup>, Lucas Sawade<sup>3</sup>, Lars Ottemöller<sup>2</sup>, and Felix Halpaap<sup>2</sup>

<sup>1</sup>GFZ Potsdam

<sup>2</sup>University of Bergen

<sup>3</sup>Princeton University

November 22, 2022

## Abstract

Over the last decades, the receiver function technique has been widely used to image sharp discontinuities in elastic properties of the solid Earth at regional scales. To date, very few studies have attempted to use receiver functions for global imaging. One such endeavour has been pursued through the project “Global Lithospheric Imaging using Earthquake Recordings” (GLImER). Building on the advances of GLImER, we have developed PyGLImER - a Python-based software suite capable of creating global images from both P-to-S and S-to-P converted waves via a comprehensive receiver function workflow. This workflow creates a database of receiver functions by downloading seismograms from selected earthquakes and analysing the data via a series of steps that include pre-processing, quality control, deconvolution, and stacking. The stacking can be performed for common conversion points or single stations. All steps leading to the creation of receiver functions are automated. To visualise the generated stacks, the user can choose the desired survey area in a graphical user interface, and then explore the selected region either through 2D cross-sections or a 3D volume. By incorporating results from two independent seismic phases, we can combine the advantages of both phases for imaging different discontinuities. This results in an increased robustness and resolution of the final image. For example, we can use constraints from S receiver function images, which are multiple-free but relatively low resolution, to differentiate between real lithospheric/asthenospheric structures and multiple-induced artefacts in higher-resolution P receiver function images. Our preliminary results agree with those from recent regional and global studies, confirming the workflow’s robustness. They also indicate that the new workflow combining P and S receiver functions has the potential to resolve global lithospheric discontinuities such as the lithosphere-asthenosphere boundary (LAB) or the midlithospheric discontinuity (MLD) more reliably than approaches using only one type of incident phase. PyGLImER will be distributed as open-source software, providing an easily accessible tool to rapidly generate high-resolution images of structures in the lithosphere and asthenosphere over large scales.

# PyGLImER: A New Modular Software Suite to Image Crustal and Upper-Mantle Discontinuities Using a Global Database of Ps and Sp Receiver Functions

Peter Makus<sup>1</sup>, Stéphane Rondenay<sup>1</sup>, Lucas Sawade<sup>2</sup>, Lars Ottemöller<sup>1</sup>, and Felix Halpaap<sup>1</sup>

<sup>1</sup>Department of Earth Science, University of Bergen <sup>2</sup>Department of Geosciences, Princeton University



PRESENTED AT:



# INTRODUCTION

## What Are Receiver Functions?

S and P receiver functions (SRF, PRF) are created by deconvolving the upgoing direct S and P phase from the Sp and Ps converted signals, respectively. The direct arrival is an approximation of the source wavelet (neglecting noise and anisotropy) and, consequently, the RF is an estimation of the medium's impulse response, with maxima located at discontinuities in seismic impedance<sup>1</sup>.

Despite having lower resolution due to their longer period, SRFs are better suited to image discontinuities in the lower lithosphere than PRFs. This is because in PRFs, the P-to-S conversions from the lithosphere are contaminated by multiples, whereas in SRFs the multiples are clearly separated from conversions (conversions before S, multiples after S)<sup>2</sup>.

**Fig. 1. Conversion of a teleseismic S-wave.** a) Vertical cross-section through the subsurface, in which an incident teleseismic S-wave (blue) is converted into an Sp wave (red) at a downwards positive impedance contrast (green) under the receiver (black triangle). b) Theoretical output of the radial (R) component of the receiver's seismogram synthetically created using a Ricker-wavelet as source-time function containing both P (red) and S (blue) wave energy. Note that the converted wave arrives earlier than the primary arrival.

## About PyGLImER

To tackle the lack of toolsets for global P-to-S and S-to-P receiver function imaging, we develop PyGLImER - a direct successor to GLImER<sup>3</sup>. Compared to its predecessor, PyGLImER introduces the following tools and advances:

- The ability to update the database without compromising existing data.
- The database can now be created from data downloaded from any FDSN compatible server.
- Inclusion of S-to-P and SKS-to-P RFs.
- A user-friendly pythonic implementation.

# DATA

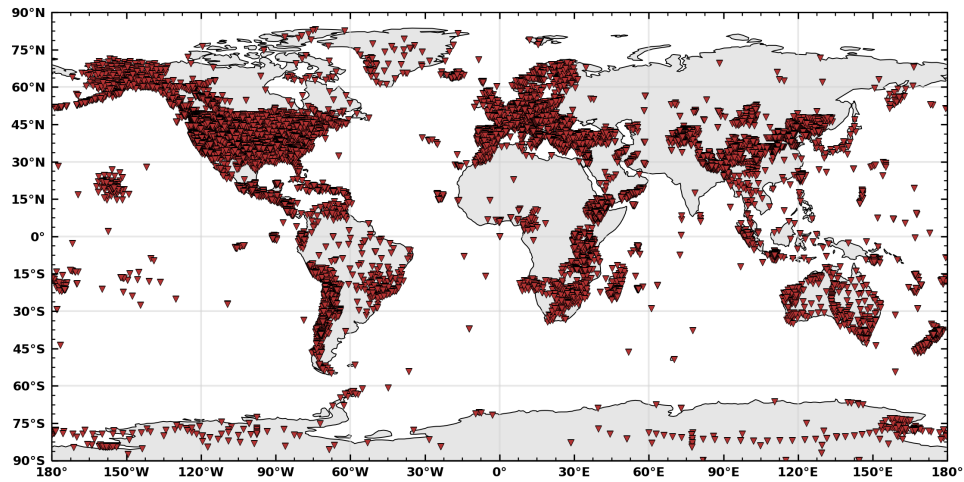


Fig. 2. Seismic broadband and very-broadband stations in the PyGLImER database. Red downward-pointing triangles are seismic stations.

Owing to the ability to access all openly available data from all FDSN servers, we can create a RF database of unprecedented extent. Our preliminary database contains recordings from **21,969 events** at **22,715 seismic broadband stations** (see Fig. 2) resulting in over **30 million raw waveforms**. After quality control and deconvolution, the database comprises more than **2 million RFs** - 1.5 million PRFs and 0.5 million SRFs (only radial RFs included. However, PyGLImER is capable of producing transverse RFs).

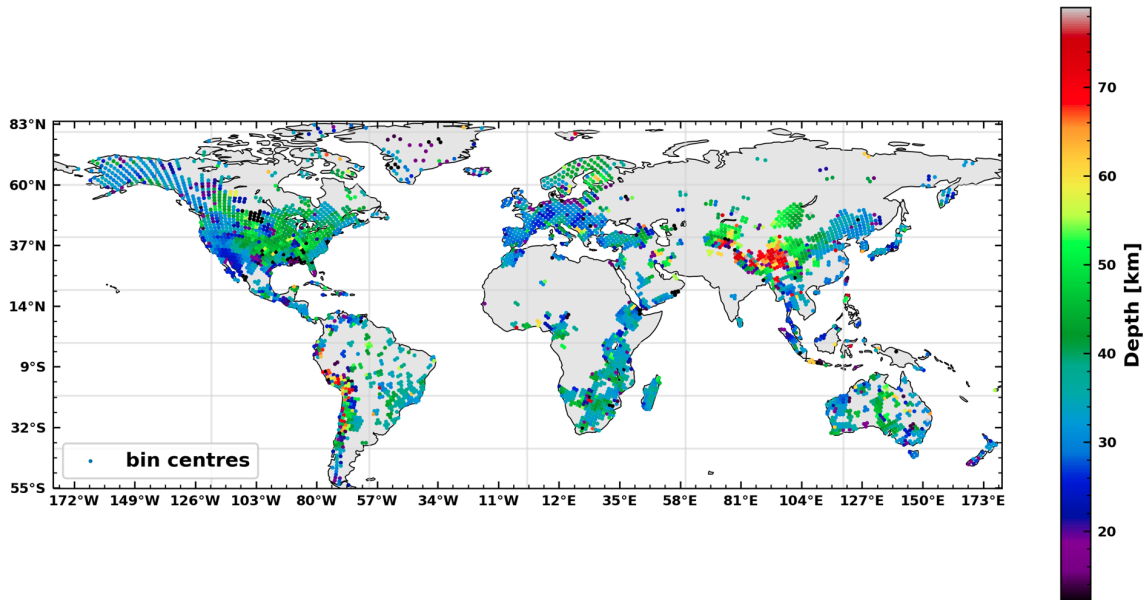
# REAL AND SYNTHETIC DATA EXAMPLES

In this panel, we show applications of our software suite to examples from real and synthetic data. More detailed descriptions of the maps and images are given in the figure captions.

## Real Data Examples

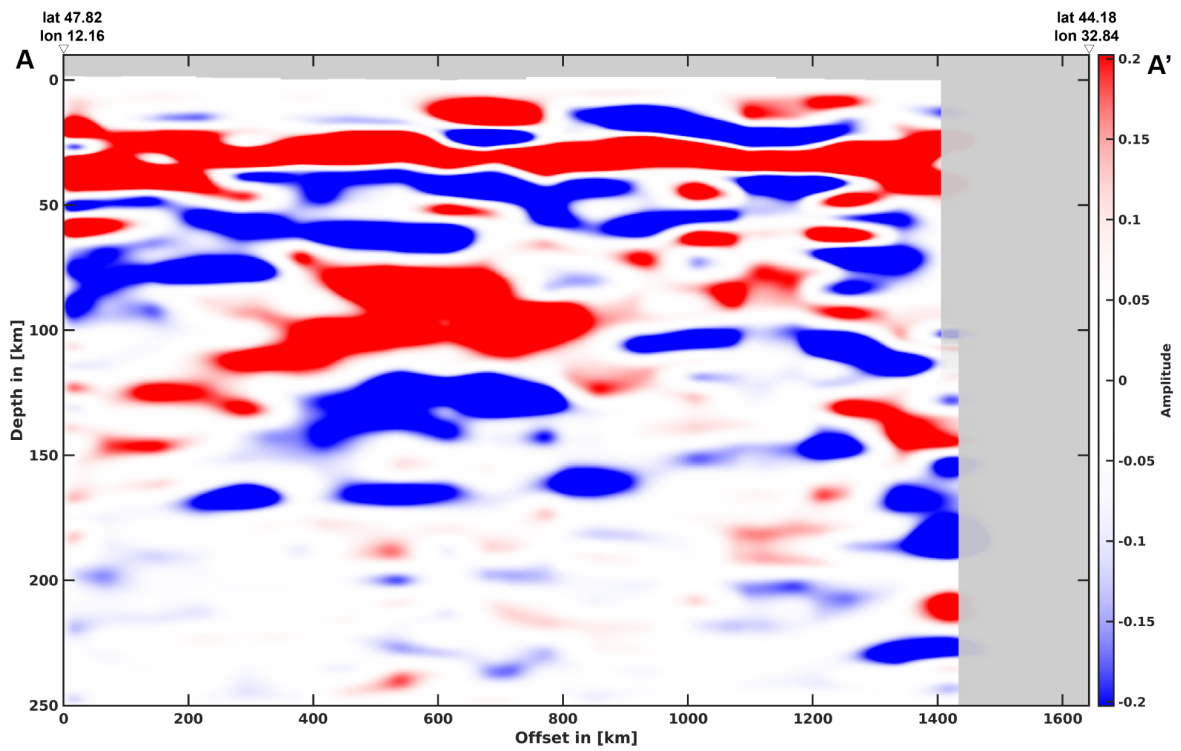
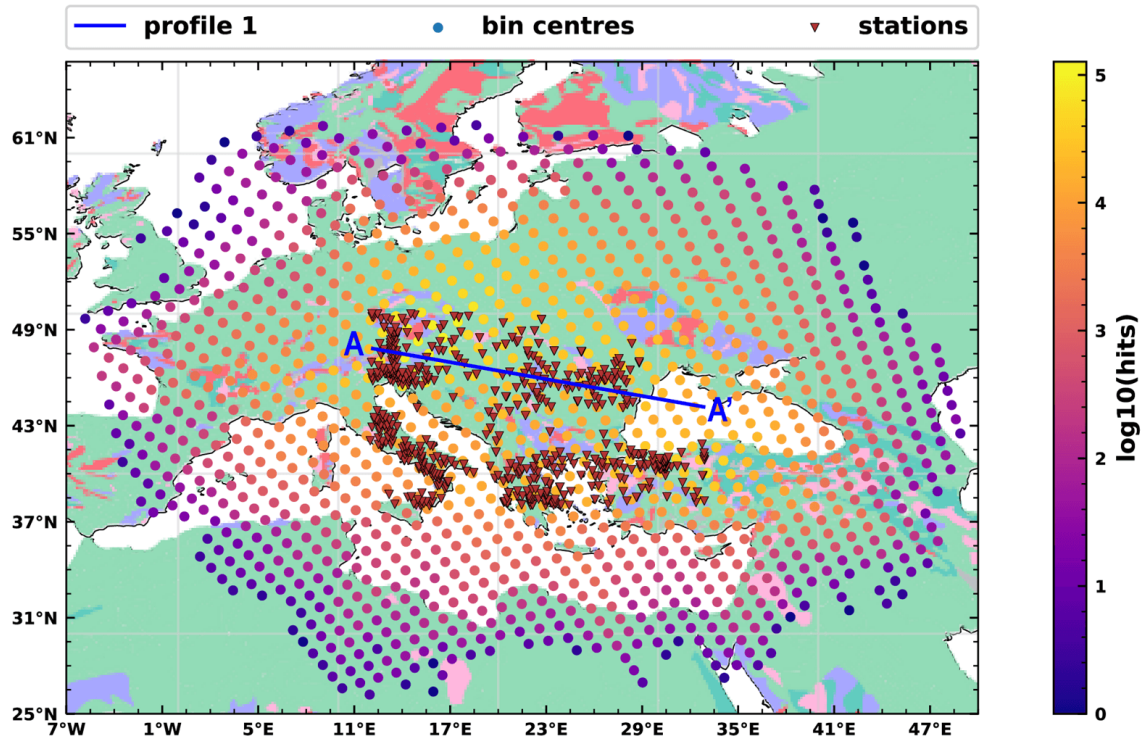
After an initial RF database is established, PyGLImER can create common conversion point (CCP) stacks for any desired region. Thereafter, the CCP objects can be visualised as maps or sections - as illustrated by the following figures.

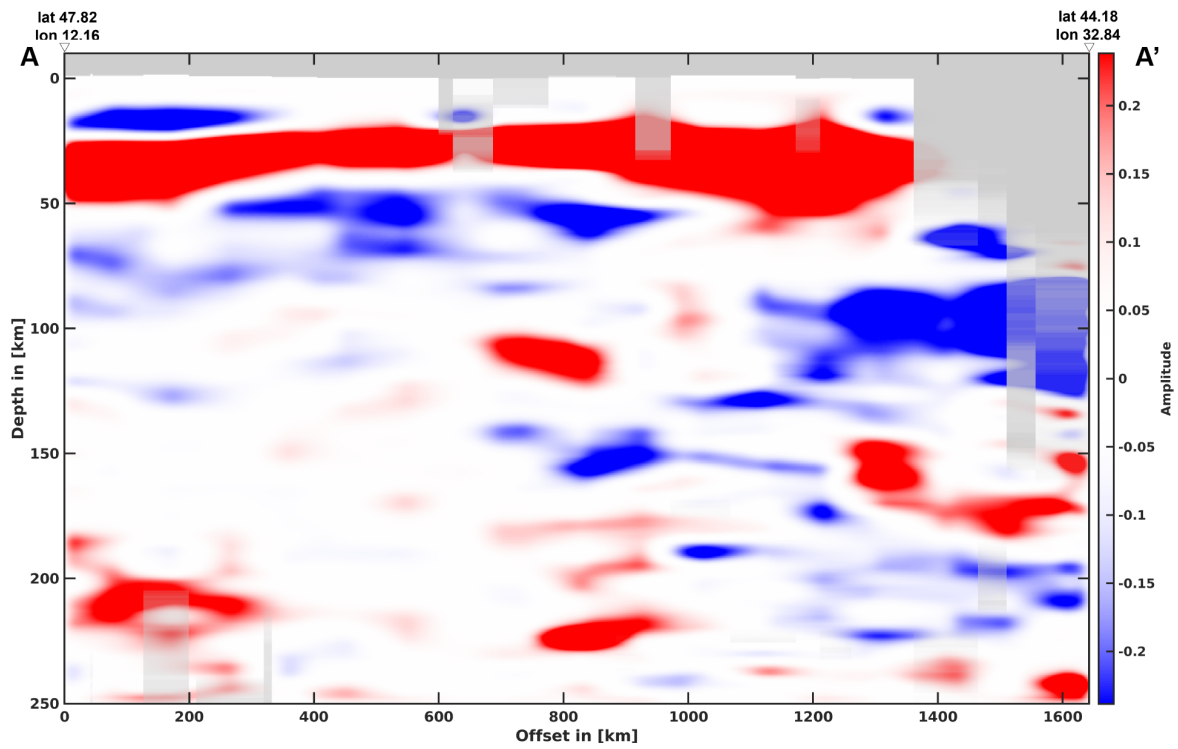
### Global Moho Depth



**Fig. 3. A global map of Moho depth.** The mapped values correspond to the depth of the maximum amplitude phase found in the PRF common conversion point (CCP) stacks between 10km and 80km depth. Bins that are insufficiently illuminated in the given depth range are automatically omitted. The function used to pick the conversion of a certain phase and the plotting function are part of the PyGLImER module.

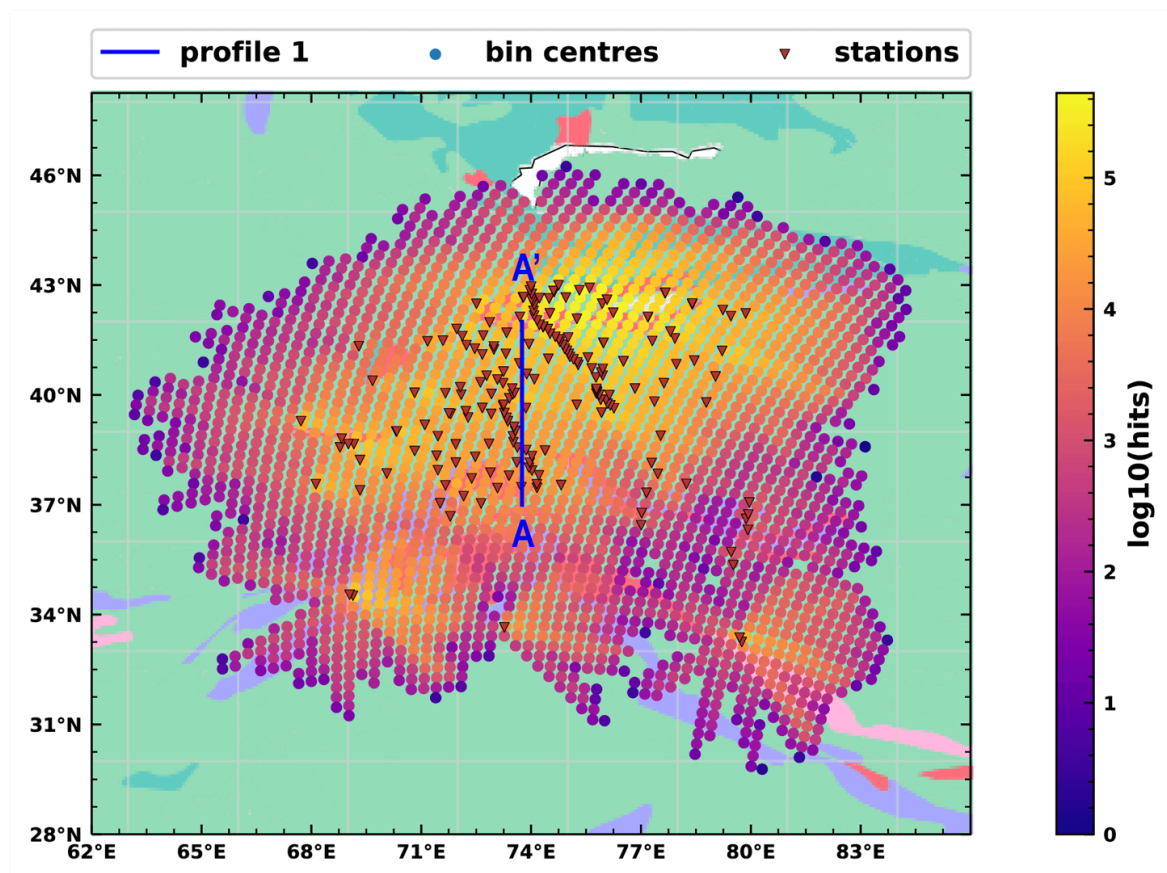
### Eastern Europe





**Fig 4. A CCP object under eastern Europe.** (Upper panel) A map view of the cross-section (blue line). Illumination is given in depth-cumulative hits per bin. (Middle panel) A cross-section through PRF data. (Lower panel) A cross-section through SRF data. In the PRF and SRF sections, data are greying out for grid points with fewer than 50 and 25 hits, respectively.

### Hindu-Kush and Pamir



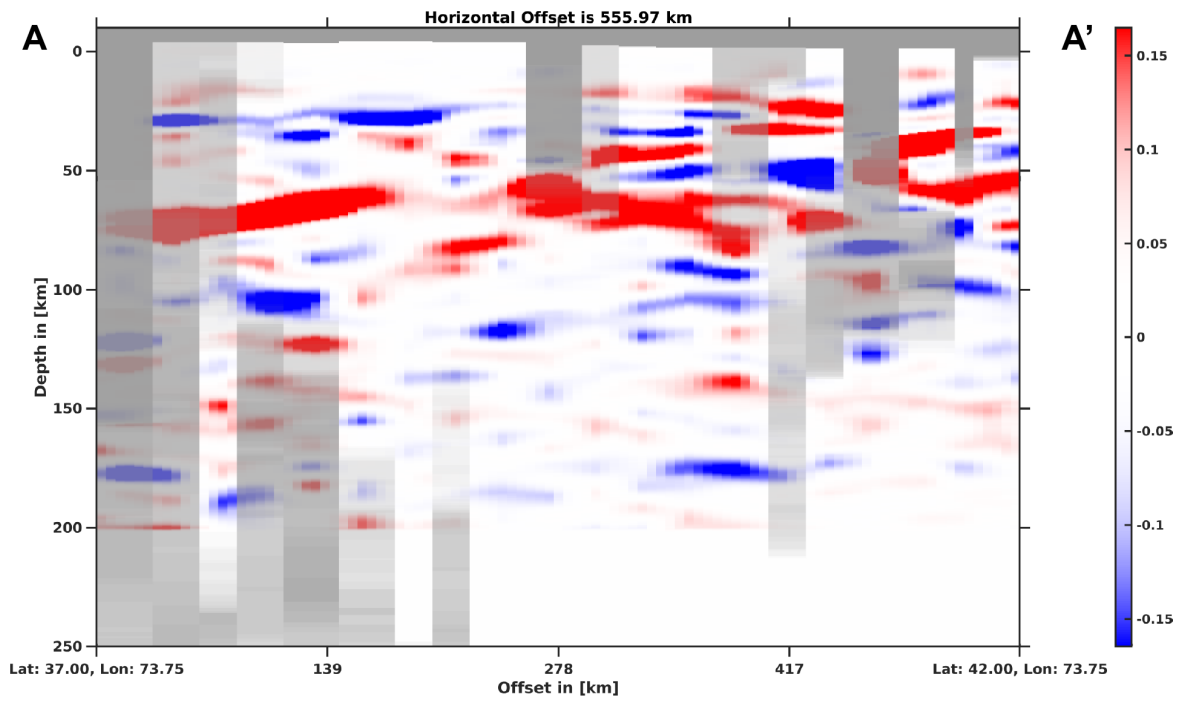
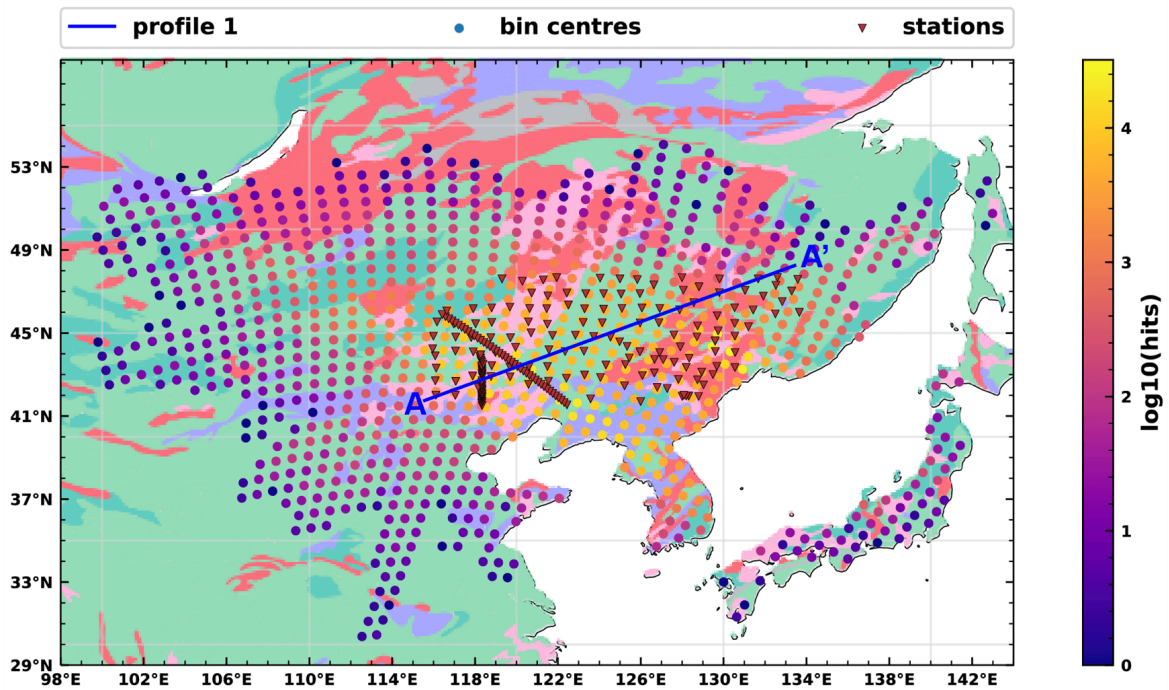
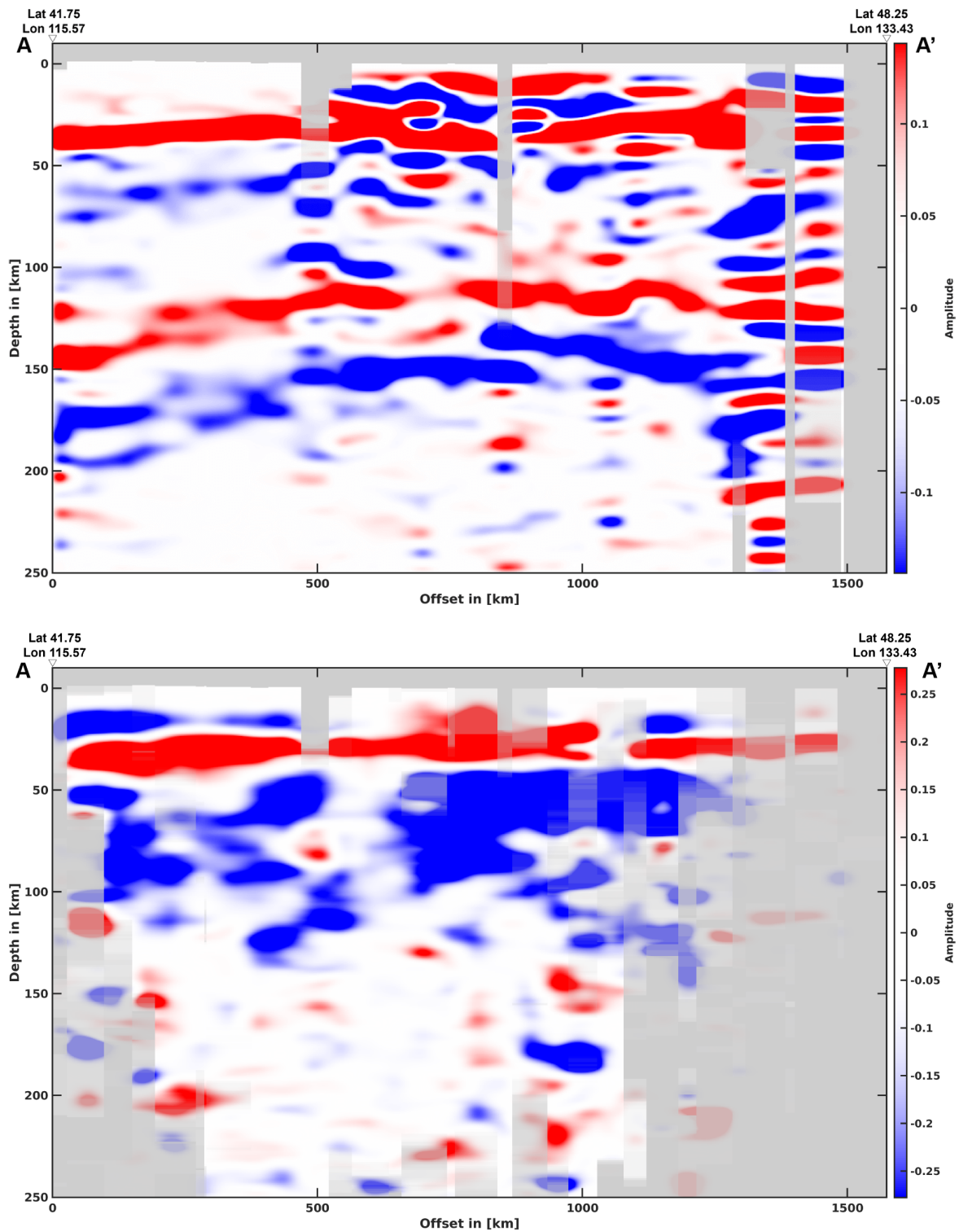


Fig. 5. A CCP object under the Hindu-Kush and the Pamir orogen. (Upper panel) A map view of the cross-section (blue line). Illumination is given in depth-cumulative hits per bin. (Lower panel) A cross-section through PRF data. Data are greying out for grid points with fewer than 25 hits.

## North China Craton





**Fig 6. A CCP object through the North China craton.** (Upper panel) A map view of the cross-section (blue line). Illumination is given in depth-cumulative hits per bin. (Middle Panel) A cross-section through PRF data. (Lower panel) A cross-section through SRF data. In the PRF and SRF sections, data are greying out for grid points with fewer than 50 and 25 hits, respectively.

## North America

Here, we demonstrate how created CCP volumes can be interactively explored for both PRF and SRF using a new pythonic tool (video 1) or an old Matlab implementation<sup>4</sup>(video 2), respectively.

[VIDEO] <https://www.youtube.com/embed/VZ1ysdlMss8?rel=0&fs=1&modestbranding=1&rel=0&showinfo=0>

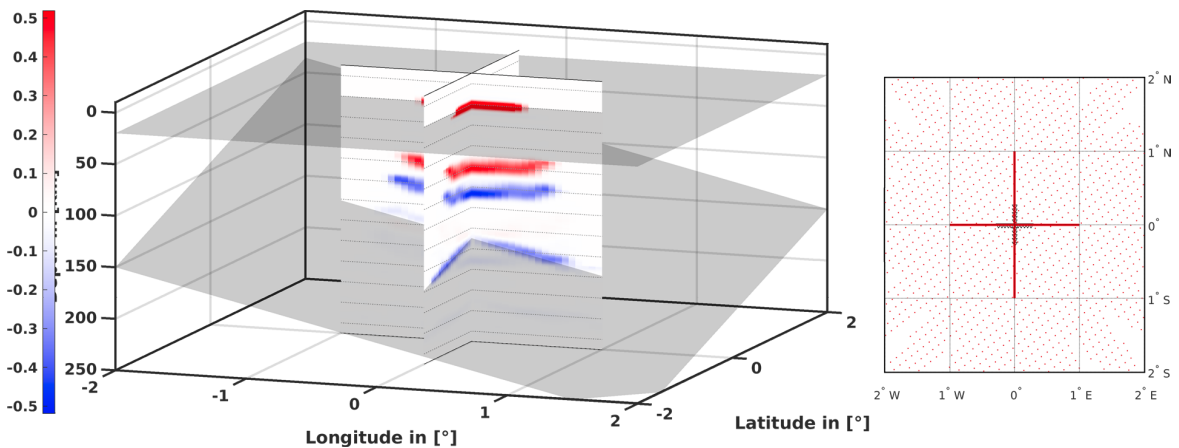
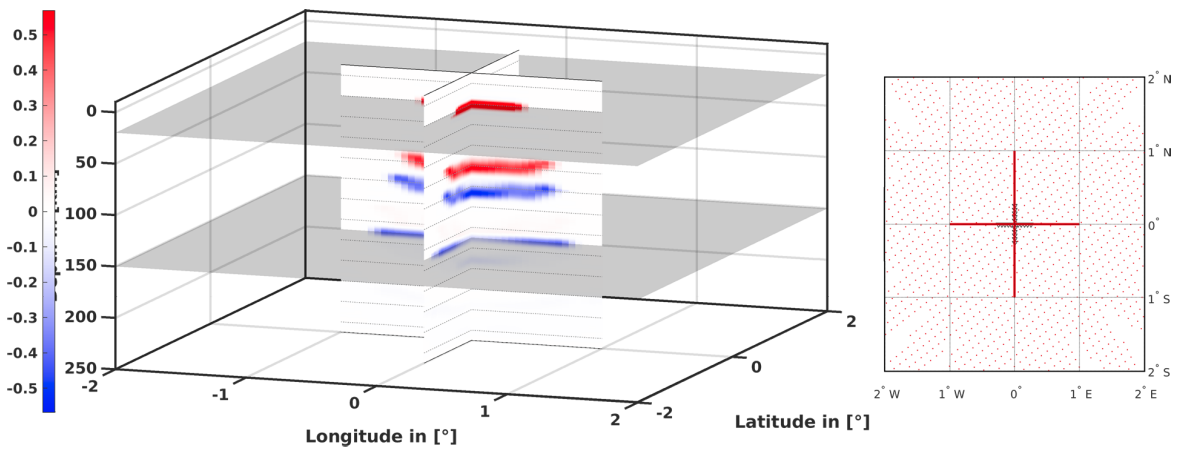
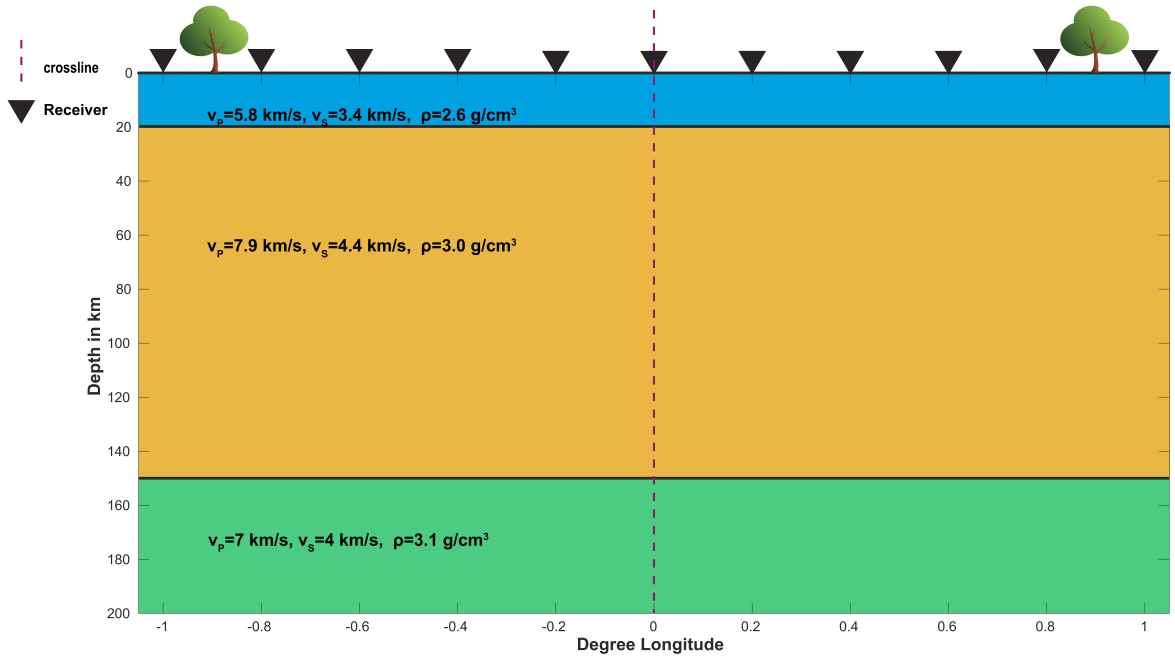
**Video 1: Exploring a CCP Volume created from PRF data under the North American continent.** A preview of a new interactive tool to explore CCP volumes in PyGLImER.

[VIDEO] <https://www.youtube.com/embed/02C-GsHEpAQ?rel=0&fs=1&modestbranding=1&rel=0&showinfo=0>

Video 2: Exploring a CCP Volume created from SRF data under the North American continent. Exploration is done in Matlab using a previous Matlab implementation<sup>4</sup>.

## Synthetic Data Examples

We used RaySum<sup>5</sup> to model incoming teleseismic P and S wavefronts. Subsequently, we invert for the used velocity model to test the method's robustness.



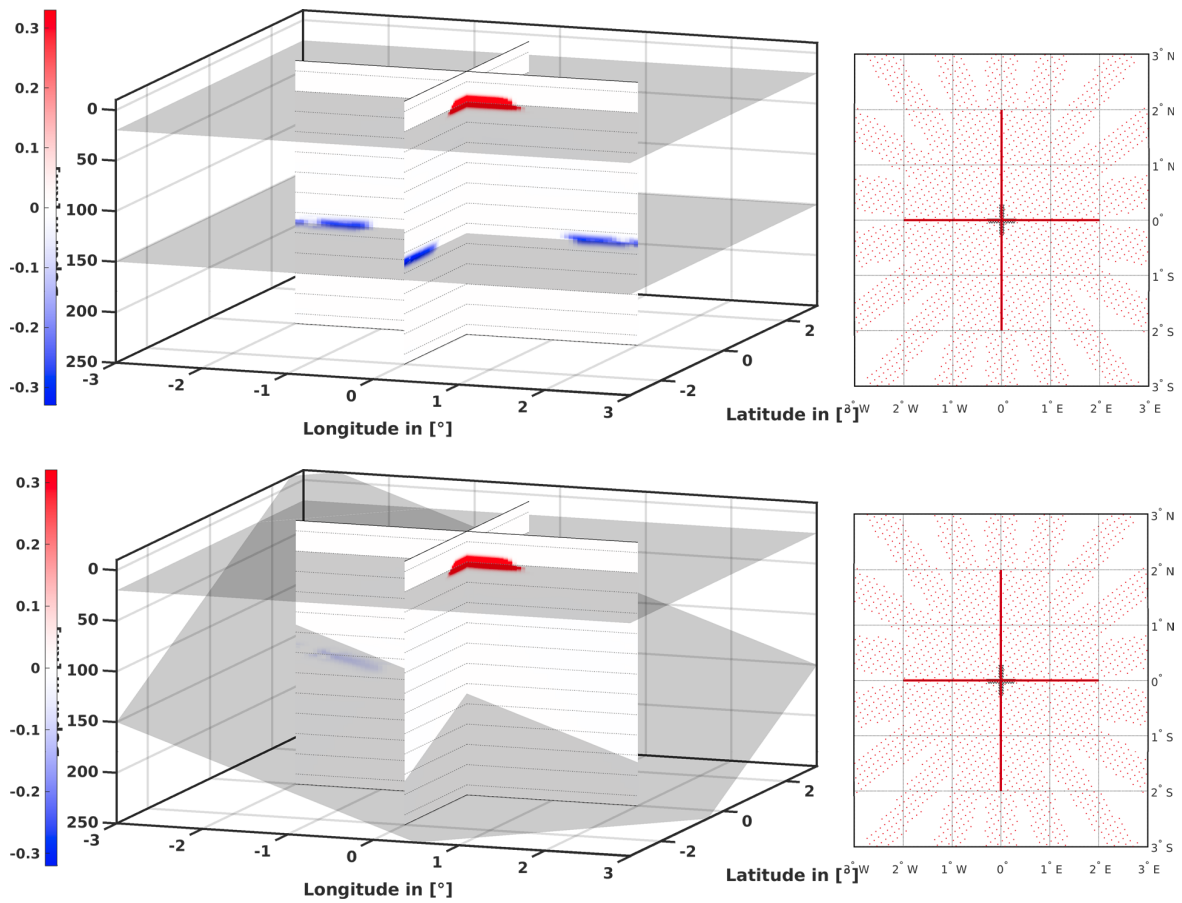


**Fig 7. CCP stacks created from synthetic RFs.** Synthetic waveforms were produced using RaySum<sup>5</sup>. (First panel) The model that was used for the forward modelling. We conducted tests with different dips and a strike of 45 degrees for the lowermost boundary. (Second panel) A CCP stack from PRF data, where all boundaries are horizontal. (Third panel) A CCP stack from PRF data, where the lower boundary dips by 20 degrees. (Fourth panel) A CCP stack from SRF data, where all boundaries are horizontal. (Fifth panel) A CCP stack from SRF data, where the lower boundary dips by 20 degrees. The traces of the boundaries are plotted as semitransparent

Note that:

- SRFs are not contaminated by multiples.
- PRFs are better suited to image dipping boundaries.
- Within the limits of illumination, 1D models are perfectly recovered.

# FUNCTIONALITIES & IMPLEMENTATION

PyGLImER creates a RF database over a comprehensive workflow (see Fig. 7). The implementation relies heavily on the obspy module<sup>6</sup>. Handling of the receiver function objects is partly carried out by the rf module<sup>7</sup>.

For deconvolution, the user can choose between three different algorithm groups:

- Iterative time domain deconvolution<sup>8</sup>
- Extended-time multitaper frequency domain cross-correlation<sup>9</sup>
- Three different approaches based on spectral division (e.g., waterlevel spectral division<sup>10</sup>)

A demonstration of PyGLImER's most essential features can be found in the Jupyter notebook linked below. All functions and features have undergone extensive robustness tests with synthetic and real data.

**[PyGLImER demo notebook \(https://nbviewer.jupyter.org/github/PeterMakus/demo\\_PyGLImER/blob/main/demo\\_notebook.ipynb\)](https://nbviewer.jupyter.org/github/PeterMakus/demo_PyGLImER/blob/main/demo_notebook.ipynb)**

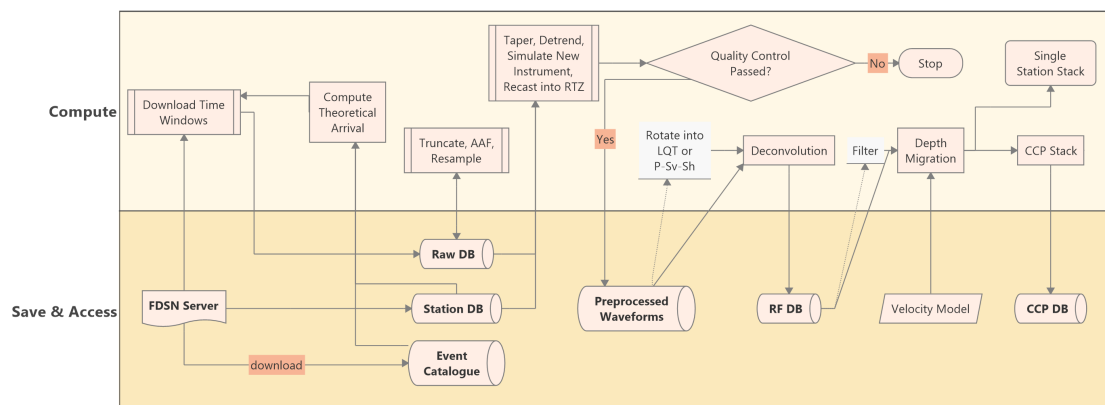


**Fig. 8.** The processing scheme of PyGLImER's receiver function workflow from a stream containing raw waveforms to the final CCP stack. A cylinder represents a local database, which PyGLImER constructs, processes with a double-boarder are fully automated, grey steps are voluntary, and single-bordered processes expect a user input that will alter the nature of the respective processing step. For the sake of clarity, the process is simplified and minor steps and branches are omitted.

## SUMMARY & OUTLOOK

- We present a PyGLImER, a Python-based program suite to create a global receiver function database requiring only a minimal amount of user input.
- Data can be stacked by common conversion points or station dependent and visualised and explored as cross-sections or volumes.
- Tests with synthetic and real data confirm the method's robustness.
- PyGLImER will be distributed as an open-source software via GitHub (<https://github.com/PeterMakus>).

## DISCLOSURES

The authors wish to thank the multitude of scientists, who contributed time and energy to acquire the data used in this project. Without open data policies and scientists working by those principles, the PyGLImER project would not have been possible. Pythonic Global Lithospheric Imaging with Earthquake Recordings (PyGLImER) and our participation in the AGU Fall Meeting was supported by the University of Bergen's Meltzer Grant.

# ABSTRACT

Over the last decades, the receiver function technique has been widely used to image sharp discontinuities in elastic properties of the solid Earth at regional scales. To date, very few studies have attempted to use receiver functions for global imaging. One such endeavour has been pursued through the project “Global Lithospheric Imaging using Earthquake Recordings” (GLImER). Building on the advances of GLImER, we have developed PyGLImER - a Python-based software suite capable of creating global images from both P-to-S and S-to-P converted waves via a comprehensive receiver function workflow. This workflow creates a database of receiver functions by downloading seismograms from selected earthquakes and analysing the data via a series of steps that include pre-processing, quality control, deconvolution, and stacking. The stacking can be performed for common conversion points or single stations. All steps leading to the creation of receiver functions are automated. To visualise the generated stacks, the user can choose the desired survey area in a graphical user interface, and then explore the selected region either through 2D cross-sections or a 3D volume. By incorporating results from two independent seismic phases, we can combine the advantages of both phases for imaging different discontinuities. This results in an increased robustness and resolution of the final image. For example, we can use constraints from S receiver function images, which are multiple-free but relatively low resolution, to differentiate between real lithospheric/asthenospheric structures and multiple-induced artefacts in higher-resolution P receiver function images. Our preliminary results agree with those from recent regional and global studies, confirming the workflow’s robustness. They also indicate that the new workflow combining P and S receiver functions has the potential to resolve global lithospheric discontinuities such as the lithosphere-asthenosphere boundary (LAB) or the midlithospheric discontinuity (MLD) more reliably than approaches using only one type of incident phase. PyGLImER will be distributed as open-source software, providing an easily accessible tool to rapidly generate high-resolution images of structures in the lithosphere and asthenosphere over large scales.

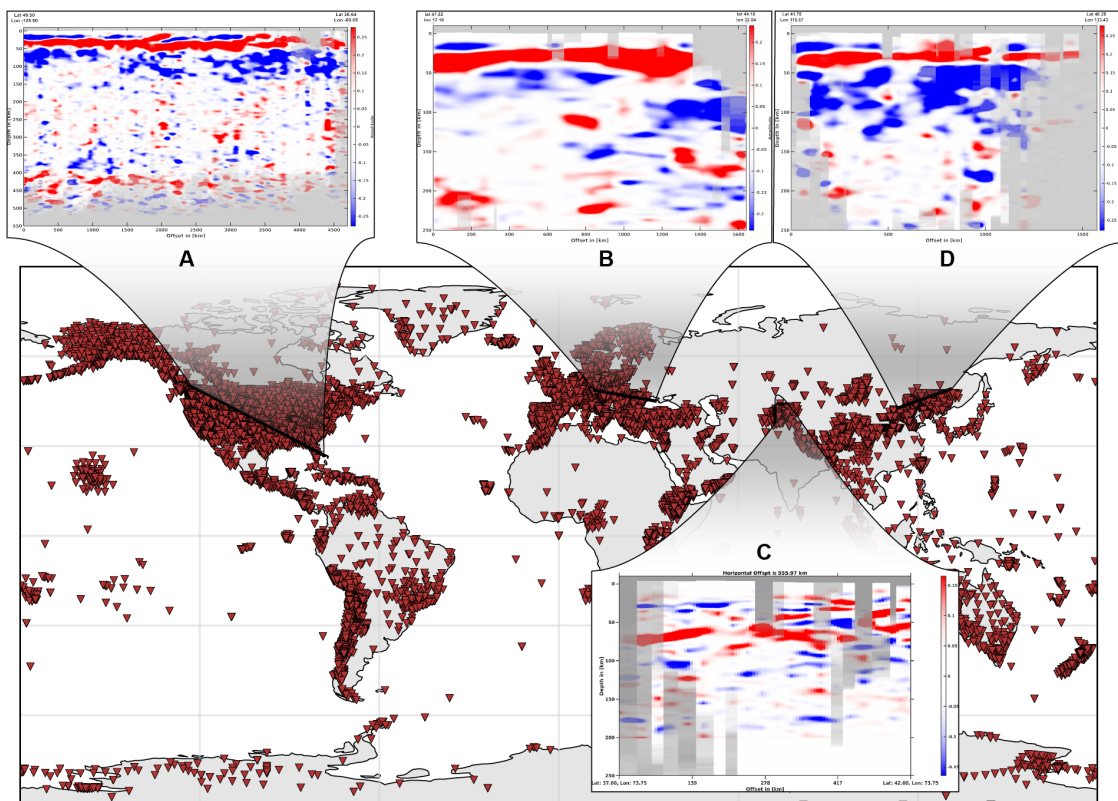


**Fig. 0. Global receiver function imaging using PyGLImER.** Seismic broadband stations with available receiver functions are plotted as downward pointing red triangles. The locations of the shown cross-sections are demarked as bold black lines. Cross-sections A, B, and D are created from S receiver functions stacked by common conversion point, whereas cross-section C shows a slice through a P receiver function common conversion point stack. Data begin to fade to grey if the respective gridpoint is hit by fewer than 25 rays. Note that the vertical exaggeration varies from panel to panel.

## REFERENCES

- <sup>1</sup>Rondenay, S. (2009). Upper mantle imaging with array recordings of converted and scattered teleseismic waves. *Surveys in geophysics*, 30(4-5), 377-405.
- <sup>2</sup>Farra, V., & Vinnik, L. (2000). Upper mantle stratification by P and S receiver functions. *Geophysical Journal International*, 141(3), 699-712.
- <sup>3</sup>Rondenay, S., Spieker, K., Sawade, L., Halpaap, F., & Farestveit, M. (2017). Glimer: A new global database of teleseismic receiver functions for imaging earth structure. *Seismological Research Letters*, 88(1), 39-48.
- <sup>4</sup>Rondenay, S., Sawade, L., and Makus, P.: GLImER: a MATLAB-based tool to image global lithospheric structure, EGU General Assembly 2020, Online, 4–8 May 2020, EGU2020-22607, <https://doi.org/10.5194/egusphere-egu2020-22607>, 2020.
- <sup>5</sup>Frederiksen, A. W., & Bostock, M. G. (2000). Modelling teleseismic waves in dipping anisotropic structures. *Geophysical Journal International*, 141(2), 401-412.
- <sup>6</sup>Krischer, L., Megies, T., Barsch, R., Beyreuther, M., Lecocq, T., Caudron, C., & Wassermann, J. (2015). ObsPy: A bridge for seismology into the scientific Python ecosystem. *Computational Science & Discovery*, 8(1), 014003.
- <sup>7</sup>Eulenfeld, T. (2020). rf: Receiver function calculation in seismology. *Journal of Open Source Software*, 5(48), 1808.
- <sup>8</sup>Ligorria, J. P., & Ammon, C. J. (1999). Iterative deconvolution and receiver-function estimation. *Bulletin of the seismological Society of America*, 89(5), 1395-1400.
- <sup>9</sup>Helffrich, G. (2006). Extended-time multitaper frequency domain cross-correlation receiver-function estimation. *Bulletin of the Seismological Society of America*, 96(1), 344-347.
- <sup>10</sup>Clayton, R. W., & Wiggins, R. A. (1976). Source shape estimation and deconvolution of teleseismic bodywaves. *Geophysical Journal International*, 47(1), 151-177.